表5　理想的なう蝕診断機器の要件

- 安全性
- 初期う蝕病巣を客観的，かつ高い信頼性で検出
- 連続観察による初期う蝕病巣のモニタリング（進行性・停止性・消失）
- う蝕活動性の評価
- EBPのための有用なデータ表示

表6　今後のう蝕学に必要な事項

1．新しいう蝕診断システムの開発
2．う蝕の自然史に基づいたう蝕学の新しい知識の確保
3．新しい予防製品の評価
4．臨床的意思決定（decision making）の理解
5．う蝕リスク評価の明示
6．ヘルスサービスとその結果の進展
7．疫学研究

4．DIFOTIによる初期う蝕の定量評価の可能性

DIFOTIのコントラストレベル強度と，TMRによる脱灰深さおよびQLFによって脱灰量を表わす面積蛍光強度との間で，図9に示すように，それぞれのパラメータ間で高い相関性が認められた（$p < 0.05$）．しかし，DIFOTIのコントラストレベル強度とTMRによる表層エナメル質の厚さおよびミネラル溶出量との間では，相関に有意性は認められなかった[10]．

一方，QLFのパラメータにおいて，平均蛍光強度とTMRによる脱灰深さ，ミネラル溶出量との間に，それぞれ高い相関性を示した（$p < 0.01$，$p < 0.05$）．また，面積蛍光強度は脱灰深さ，ミネラル溶出量との間に有意の相関が認められた（$p < 0.05$）[10]．

以上のことから，DIFOTIはQLFと比較して初期う蝕の検出感度は同じようであるが，定量評価において，初期う蝕病巣を的確に表すことができなかった．臨床応用できるように，さらなる今後の研究成果と開発が待たれるところである．

まとめ

今後のう蝕学に必要な事項（表5・表6）[11]を踏まえ，早期う蝕診断は科学に基づく効率のよいう蝕予防に必要不可欠であることを再確認するとともに，早期う蝕診断を下せる診断機器がより改良され，近い将来臨床で十分応用されることを期待している．

文献

1）Drirks OB：Posteruptive changes in dental enamel, J. Dent. Res. 45：503—511, 1966.
2）上村参生，神原正樹，本山正治，大東道治：原子間力顕微鏡による乳歯エナメル質の表面微細構造の観察，歯科医学，64：299—305，2001.
3）神原正樹編集：The Art of Oral Health—口腔衛生学の基本技法—（第2版），学建書院，東京，2002.
4）Stookey GK：Practical applications of early caries detection methods.：in Stookey GK. edit. Early Detection of Dental Caries, Indiana University School of Dentistry：357—363, USA. 2000.
5）de Josselin de Jong EJ, Sundrom F, Westerling H, Tranaeus D, ten Bosh JJ, Angmar-Mansson B：A new method for in vivo quantification of changes in initial enamel caries with laser fluorescence, Caries Res. 29：2—7, 1995.
6）Ando M, Hall AF, Eckert GJ, Schemehorn BR, Analoui M, Stookey GK：Relative Ability of laser fluorescence techniques to quantitate early mineral loss in vitro., Caries Res. 31：125—131, 1997.
7）Eggertsson H, Analoui M, van der Veen MH, Gonzalez-Cabezas C, Eckert GJ, Stookey GK：Detection of early interproximal caries in vitro using laser fluorescence, dye-enhanced laser fluorescence and direct visual examination, Caries Res. 33：227—233, 1999.
8）Schneiderman A, Elbaum M, Shultz T, Keem S, Greenebaum M, Driller J：Assessment of dental caries with digital imaging fiber-optic transillumination (DIFOTI)：in vitro study., Caries Res. 31：103—110, 1997.
9）Zero D, Mol A, Roriz CS, Spoon M, Jacobs A, Keem S, Elbaum M：Caries detection using degital imaging fiber-optic transillumination (DIFOTITM)：A preliminary evaluation.；in Stookey GK. edit.：Early Detection of Dental Caries, Indiana University School of Dentistry：169—183, USA. 2000.
10）上村参生，土居貴士，大塚秀人，田中秀直，三宅達郎，神原正樹：DIFOTI™を用いた乳歯初期う蝕病巣の分析，日本口腔衛生学会，52：654—655，2002.
11）上村参生，神原正樹：乳歯齲蝕形成パターン，デンタルダイヤモンド，27：58—63，2002.

予防歯科へのテクノロジー

－齲蝕予防における早期齲蝕診断－

神原正樹

日本歯科医師会雑誌 第56巻第７号 別刷
（平成15年10月）

論文番号 02

SCIENCE
サイエンス

KEEP 20 TEETH TILL YOUR 80

予防歯科へのテクノロジー
―齲蝕予防における早期齲蝕診断―

神原　正樹

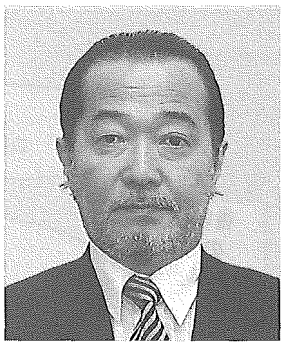

かんばら　まさき
●大阪歯科大学口腔衛生学講座教授　●歯学博士　●1972年大阪歯科大学卒業，同大学大学院修了後，大阪歯科大学口腔衛生学講座講師を経て，米国ならびにオランダへ留学。93年より大阪歯科大学教授，01年より同・大学院研究科科長，03年1月～International Association for Dental Research Cariology Group President　●1947年10月　生まれ，京都府出身　●主研究テーマ：口腔保健の確立，歯科疾患の予防など　●主な著書：臨床家のための口腔衛生学，スタンダード口腔保健学ほか

要　約

21世紀の歯科医療が住民主体の歯科疾患予防や口腔の健康増進に向かっていることは，明らかである。この方向性に沿った技術，齲蝕に対する予防や健康増進のためのEvidence-basedな技術，早期齲蝕検出が注目を集めている。QLF法は他の早期齲蝕検出法とは異なる特徴を有しており，得られた興味深い結果を本稿に示す。早期齲蝕検出法は，歯の健康を獲得するための各種方面に影響を及ぼす可能性を保持し，歯科医療がEvidence-basedな健康保持・予防へ転換するきっかけになる。

キーワード
齲蝕／診断／フッ素

1．まえがき

21世紀の歯科医療が住民主体の歯科疾患予防や口腔の健康増進に向かっていることは，齲蝕が顕著に減少し，目に見えない歯科疾患が増加し，これまでの歯科領域になかった住民の歯科に対する需要が増加しているなど歯科疾患構造や歯科医療への需要構造が変化し，さらに，近年の8020推進事業への支援強化，健康日本21・健康増進法の設立・制定など，歯科医療を取り巻く社会構造も急速に変化していることなどの背景を見れば明らかである。

これまでの歯科医療界の構図は，中心に位置する歯科医師に住民が口腔疾患の治療を依存し，この関係を歯科医師会・歯科産業・大学等が支援する構造であったのに対し，これからは口腔の健康を望む住民が中心に位置し歯科医師・歯科医師会・歯科産業・大学等が共同して住民の歯科疾患予防や健康への取り組みを支

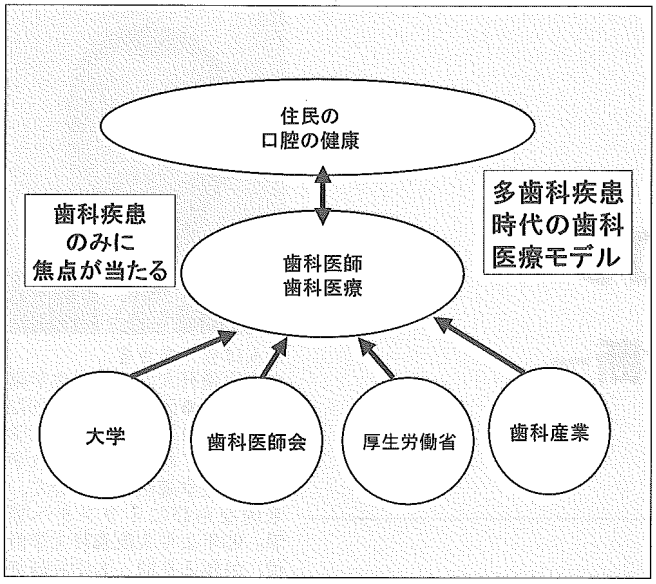

図1　これまでの歯科医療界の構造（多歯科疾患時代の歯科医療モデル）

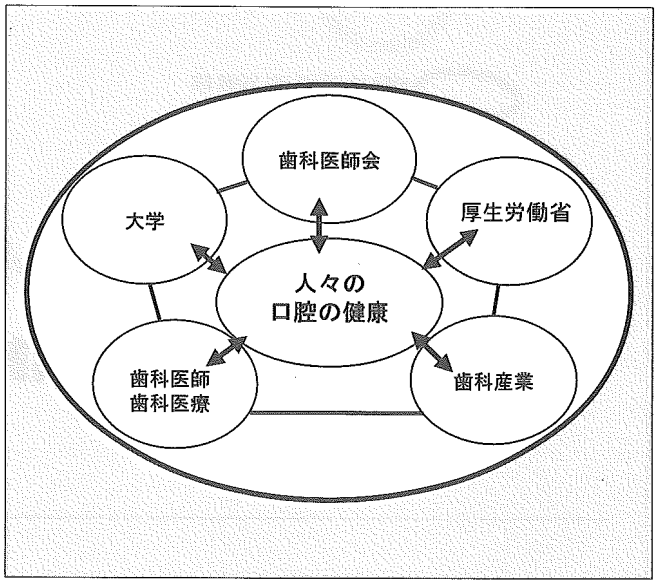

図2　21世紀の少歯科疾患時代の口腔の健康を目指した歯科界モデル（1億2千万人）

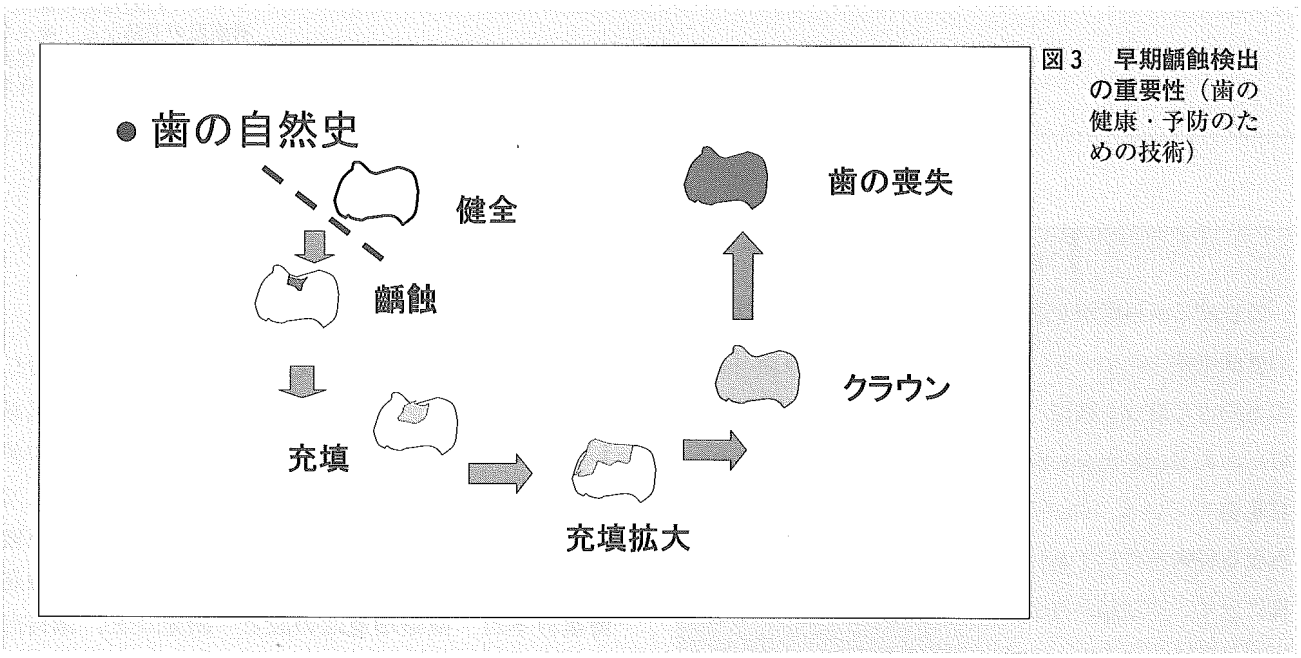

図3　早期齲蝕検出の重要性（歯の健康・予防のための技術）

援する体制に移行させていくことが必要である。この構造変化への理念は，多歯科疾患時代における治療中心の時代から，1億2千万人住民の口腔の健康を支援する歯科界への変化であり，この変化への対応を社会から迫られている構図である（図1，図2）。

このような急激な歯科医療を取り巻く社会環境が変化してきていることに，歯科界はどのような歯科医療を創造するのであろうか？　一般医療では，10年前の技術や医学が10年後には通用しなくなってきているほど急速なScienceやTechnologyの進展があるようである。歯科医療が歯科疾患予防や健康増進に向かっているとするならば，この方向性に沿った技術開発を進

展させることが肝要である（図3）。その中で，齲蝕に対する予防や健康増進のためのEvidence-basedな技術が出現し始めており，早期齲蝕検出が注目を集めている[1,2]。

2．早期齲蝕検出は何故必要なのか？

これまでの歯科医療の対象は疾患であり，21世紀の歯科医療が口腔の健康や口腔疾患の予防を目指そうとすると，健康と健康から疾患までの進行過程の把握が必要である。齲蝕予防のための真の技術的開発が望まれている。これまでの齲蝕予防は，齲蝕が出現すれば齲蝕予防不成功，出現しなければ齲蝕予防成功といい，健全エナメル質から初期齲蝕（early caries）までの変化の過程をモニターできておらず，真の齲蝕予防が実践されていなかったのが現状である。そこで，Caries prevention is invisible（齲蝕予防は見えない）からCaries prevention is visible（齲蝕予防が見える）への変遷を行おうというのが早期齲蝕検出の意味である。この流れは，保存学がConservative DentistryからPreservative Dentistryへ，Minimum Interventionなどとも並行する方向であり，齲蝕予防の3段階，第一次予防（発生予防），第二次予防(進行予防)，第三次予防(再発予防)の第一次予防重視に位置する。

海外では最近齲蝕研究に対するコンセンサス・ワーク（ICW-CCT；International consensus Workshop on Caries Clinical Trials[3]，NIH Consensus Development Conference on Dental Caries[4]，ICDAS）が盛んであり，その場で，齲蝕に関連する言葉が定義付けられているので紹介しておく。

◇Caries Lesion（齲蝕窩洞）：ある時点における齲蝕の進行段階を表す

◇Caries Process（齲蝕進行）：Biofilm，歯表面，表層下エナメル質の相互作用として生じる

◇Caries Detection（齲蝕検出）：齲蝕があるかどうかを決定する客観的方法

◇Caries Assessment（齲蝕評価）：検出後の齲蝕の特性あるいは監視を目的としたもの

1）Progression of Caries（齲蝕進行性）：深部に拡がろうしている状態にある齲蝕

2）Arrestment of Caries（齲蝕停止性）：進行しない状態にある齲蝕

3）Regression of Caries（齲蝕回復性）：健全に戻ろうとしている齲蝕

◇Caries Diagnosis（齲蝕診断）：有効なすべてのデータを専門的，客観的に，将来予測を含めて判断すること

これまでの日本で使用されてきた齲蝕に関する表現，齲蝕活動性，齲蝕抵抗性，齲蝕感受性などは口腔全体から齲蝕の状態を評価することを意味していたが，実際には評価できていなかったように見える理由は，齲蝕発生多要因の中の，ホスト因子，歯がとらえられていなかったことによる。しかし，Technologyの進歩により，前記言葉はより詳細に，科学的に齲蝕を表現しようとしており，言葉の意味からも，齲蝕減少期に適応する技術が生じているようである。

齲蝕の進行段階とケアとの対応を齲蝕の氷山（アイスバーグ）として，またvisible齲蝕診断レベルを示したPittsの図4，図5を示す[5,6]。齲蝕予防のために初期齲蝕さらにはVery Early Cariesへの対応が今後ますます進んでいくようである。

今後の早期齲蝕検出に必要なこととしては，齲蝕に関する言葉の定義の明確化，患者へのEvidence-basedな齲蝕予防効果の提示，疫学および公衆衛生，臨床研究，臨床への導入，齲蝕学教育の必要性などをあげることができる。

3．現在開発されている早期齲蝕診断法

非侵襲性であることはもちろんであるが，TMRなどのエナメル質内部での表層下脱灰との相関性，再現性や，脱灰状態の定量化，さらには画像表示ができることなどが早期齲蝕検出法に要求されている[7]。現在開発をされているあるいは商品化された早期齲蝕検出技術を表1に示す[8~17]。個々技術の検出原理は異なるが，長年にわたり研究されてきた継続性が今日の使用できる技術となって実を結んできている。また，歯表

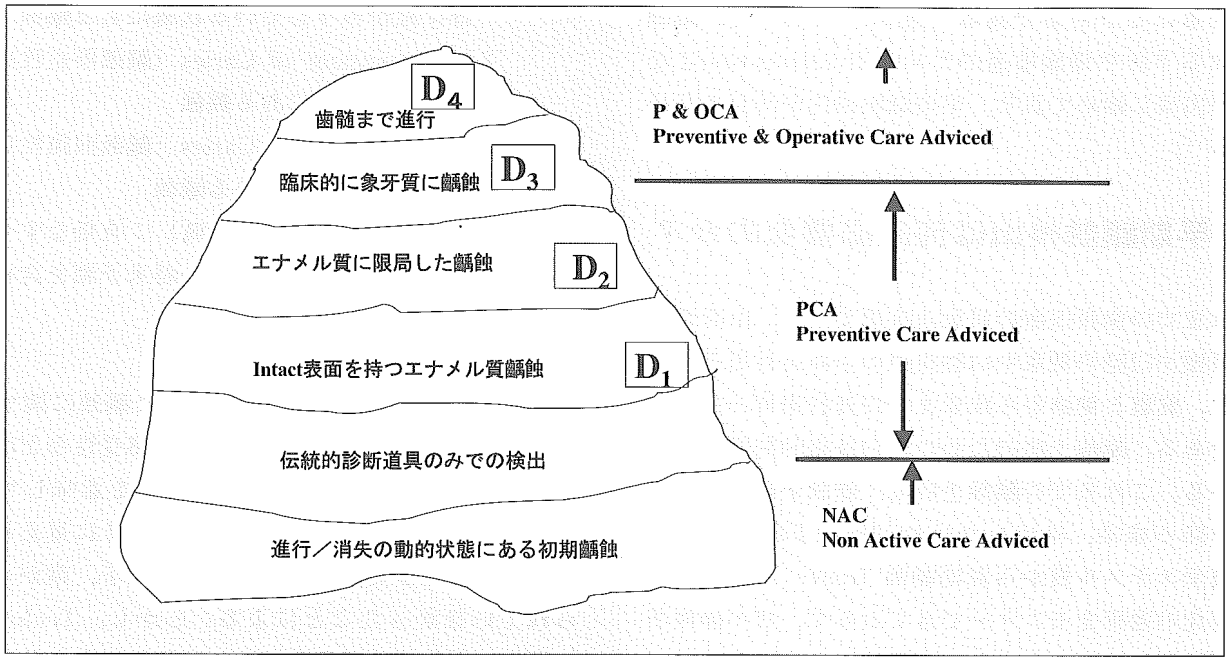

図4　齲蝕の氷山（患者への説明と治療の必要性）

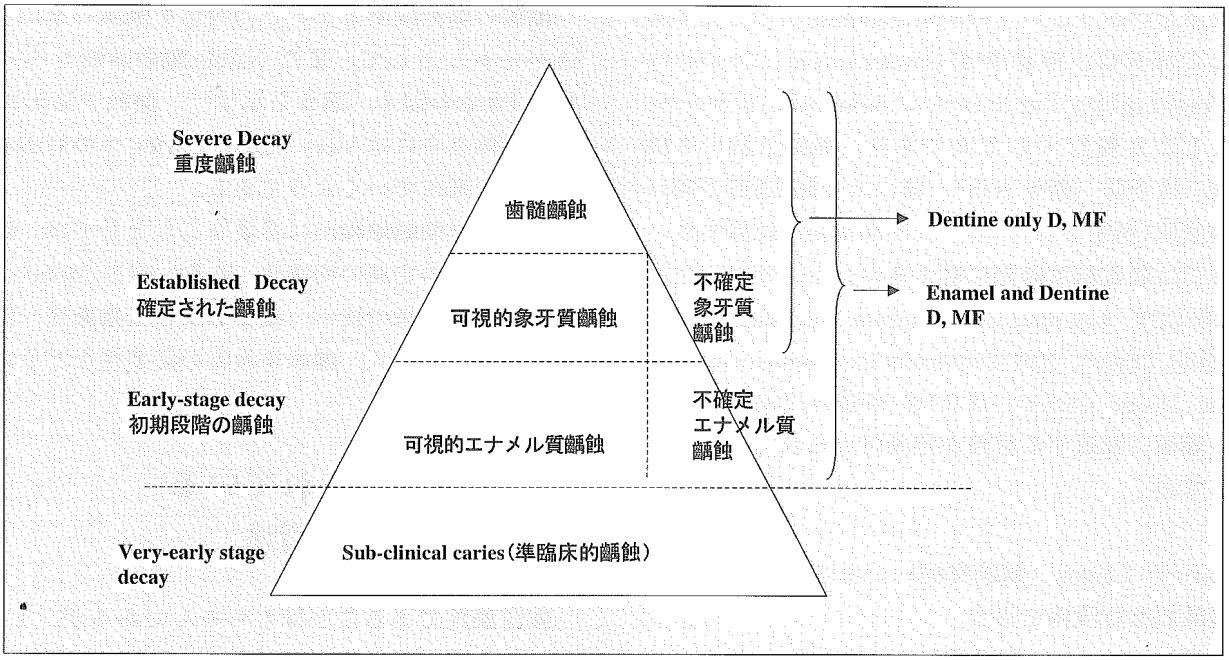

図5　Visible 齲蝕の診断レベル

面の脱灰・再石灰化現象を口腔内唾液・歯垢（バイオフィルム）・エナメル質の相互作用として追求してきた齲蝕研究の成果でもある（図6）。

個々の技術の詳細は，本稿では紙面の関係で記述できないが，平成15年7月に行われた第50回のORCA（ヨーロッパ齲蝕会議）記念大会では，再現性，定量

表1　早期齲蝕検出法

検出名称	検出原理	主な検出部位	特性値
電気抵抗値	脱灰により歯質の空隙が増加。その部位が電解質の液で満たされる。その結果，歯質の電気抵抗値が低下する現象に基づく。	咬合面 根面	深さ
FOTI 法	脱灰によりエナメル質の空隙（不連続面）が増加。その結果，光透過性が減少する現象（光の散乱）に基づく。	隣接面	深さ　広がり
Diaganodent 法	脱灰歯質に存在する，主に細菌由来の蛍光物質に赤色レーザーを照射し，その励起蛍光を計測して齲蝕を検出。	咬合面	深さ
QLF 法	特定波長の光を照射したときの歯質の励起蛍光現象に基づく。脱灰が存在すると，エナメル質内で増加した空隙（不連続面）により励起蛍光が散乱され，その検出強度が健全部位と比較して低下する。その低下度から脱灰程度を定量化。	平滑面 咬合面	深さ　面積 脱灰体積
超音波法	齲蝕により，歯質中にミネラルの密度差が存在すると，超音波はそこで反射される。反射された音波を計測することで，齲蝕の到達部位（深さ）を推定する。	隣接面 平滑面	深さ
赤外線カメラ法	初期齲蝕中の水分の気化による温度低下を超高感度赤外線カメラで計測する。	平滑面 咬合面	深さ　面積 脱灰体積

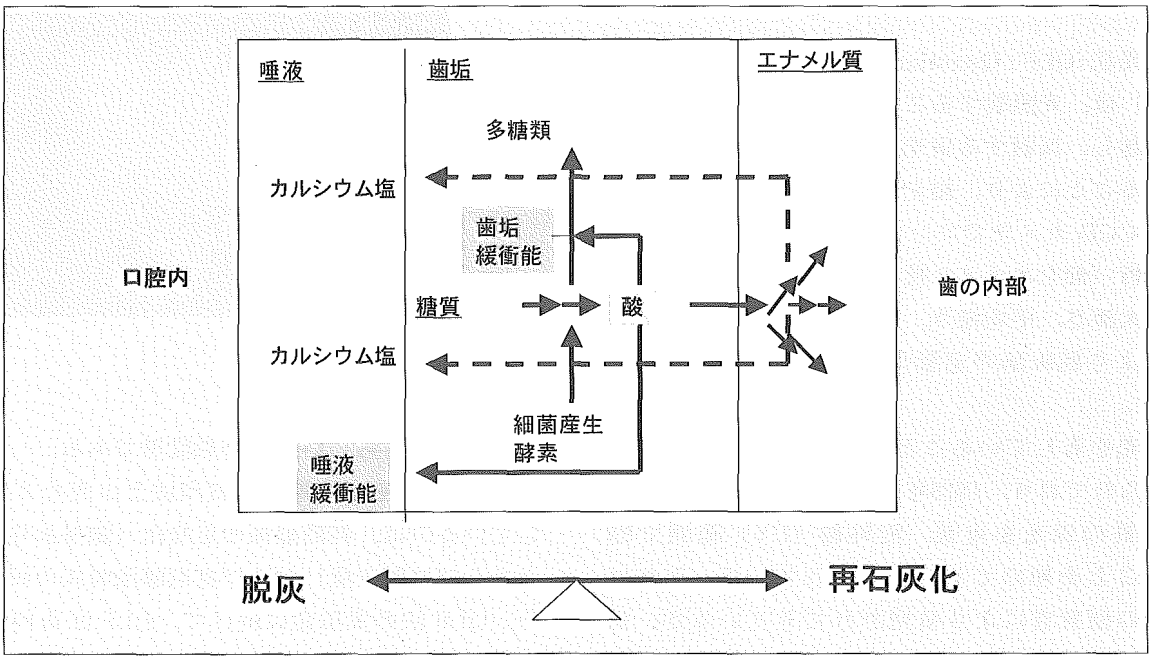

図6　唾液・歯垢・エナメル質の相互作用

化精度，画像表示などの点で，QLF 法が優れている報告が多く見られた。なお，日本版 ORCA を目指し，Cariology Today（日本齲蝕会議）が齲蝕学術研究活動を行っているため，ご参加されんことをお願いいたします。

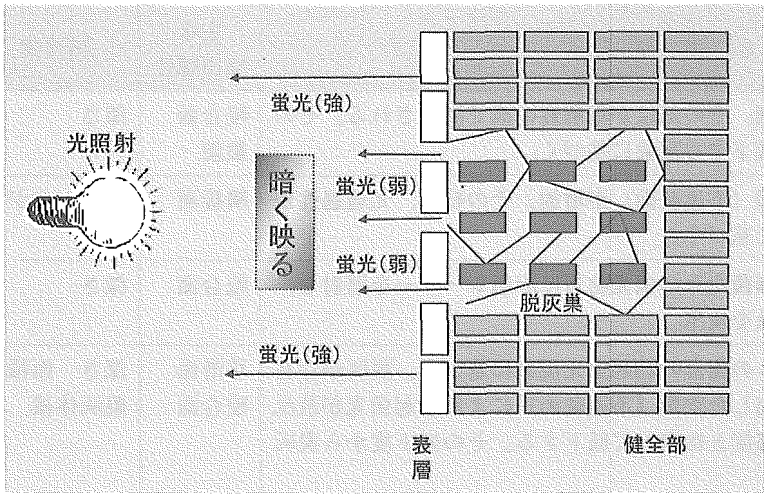

図7　定量蛍光法（QLF法）初期齲蝕検出原理

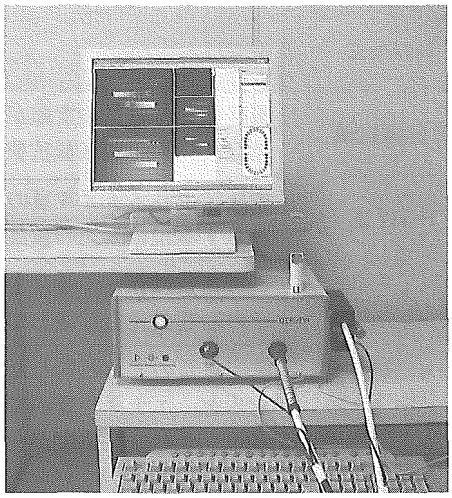

図8　定量蛍光法(QLF法)の分析機器

4．QLF法について

定量蛍光法(QLF；Quantitative Light-induced Fluorescence）は，光照射することによって歯の保有する蛍光を励起し，反射する蛍光が表層下脱灰部において乱反射することにより，健全部との差を，フィルターを通してCCDカメラでコンピューターに取り込んだ画像を解析（健全エナメル質との比較で判断し，脱灰面積，最大深さ，平均深さ，脱灰量として数値化）することにより脱灰部の定量化を図るものである（図7，図8）。

図9　歯の蛍光

歯が蛍光を有していることは（図9），歴史的に古くから知られており，1926年Benedict[18]が，エナメル質，象牙質の蛍光を可視，紫外線（UV）範囲で励起できることを初めて示したとされている。それ以来，多数の研究者により研究されてきているが，蛍光物質の特定にはいまだいたっていない。1963年Armstrong[19]は象牙質の蛍光は各種無機物質と有機物質の複合体であると示唆し，1980年Foteman[20]は象牙質の蛍光物質がアミノ酸tryptophanと未知物質であると報告し，1976年Spitzer & ten Bosh[21]はエナメル質の蛍光物質は有機物質であるなどの報告があるが，有機物であるらしいとの認識段階である。

QLF法が他の早期齲蝕検出法とは異なる特徴を有しているのは，初期齲蝕の定量化（齲蝕面積，脱灰深さならびに脱灰量）および初期齲蝕脱灰の画像化である。QLF法の実用化に向けて，QLF法有用性の研究を進めている段階であるが，得られた興味深い結果を以下に示す[21~23]。

QLF法を用いた臨床研究（1年間）の結果を示す。コントロールとしてみた齲蝕，なんらの介入をしない自然状態での1年間の推移は，初期齲蝕の進行は，進行（図10）・停止・回復（図11）それぞれであ

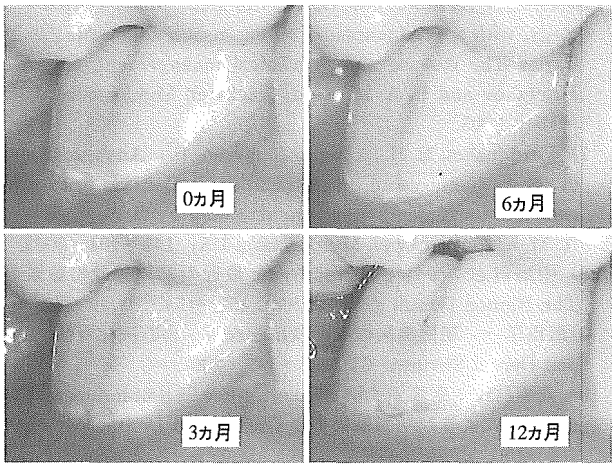

図10　初期齲蝕1年間の進行状態

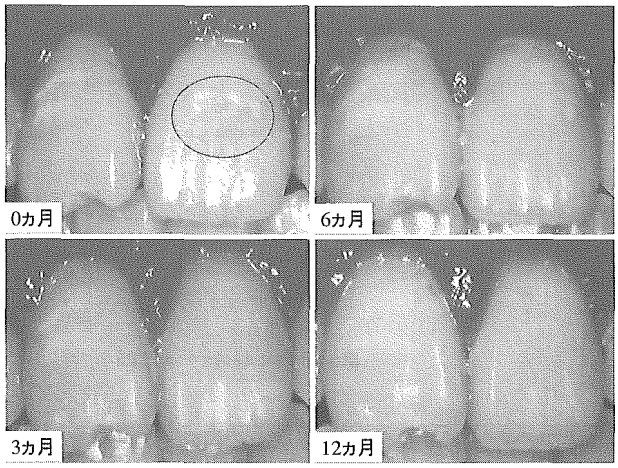

図11　初期齲蝕1年間の回復（再石灰化）状態

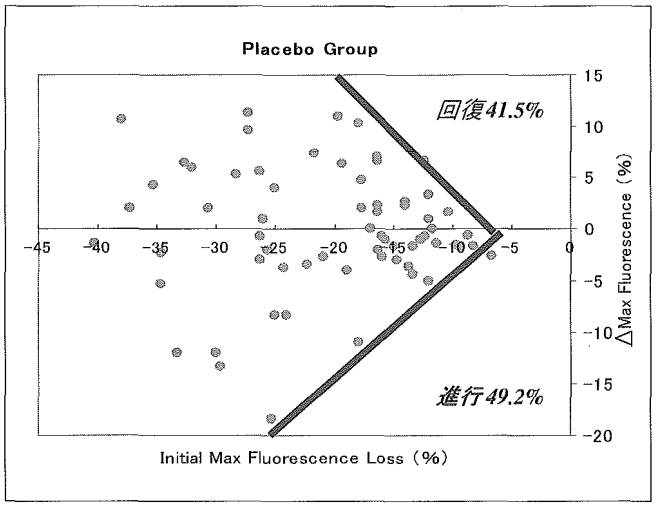

図12　コントロール群の12ヵ月後のΔmaxの分布

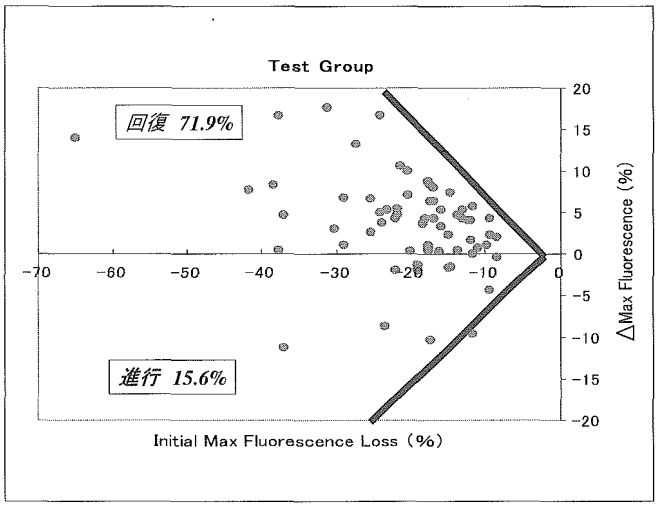

図13　フッ素配合歯磨剤群の12ヵ月後のΔmaxの分布

る。図12は，コントロール群におけるQLF法のΔmaxの初期値（横軸）から12ヵ月後の変動を示している。齲蝕が進行した初期齲蝕は49.5%，齲蝕が回復（再石灰化）した初期齲蝕41.5%であった。回復（再石灰化）をする初期齲蝕が半数見られること，口腔内での人間の自然回復能には驚きを覚える。

一方，ある種のフッ素配合歯磨剤を指示した初期齲蝕は，1年後71.5%の回復を示した（図13）。これまで報告されてきたフッ素配合歯磨剤の齲蝕抑制効果は，30〜40%程度であった結果と比較すると非常に高い齲蝕抑制率である。齲蝕検出を視診で行ってきた方法とQLF法の定量化による齲蝕検出との精度の違いを示したものと考えられる。図14は，QLF法ΔQ（脱灰量）のコントロール群とフッ素配合歯磨剤群の経日的（0，3，6，12ヵ月後）変化を示したものである。フッ素配合歯磨剤群のΔQは，3ヵ月以降，有意に回復（再石灰化）した結果であった。

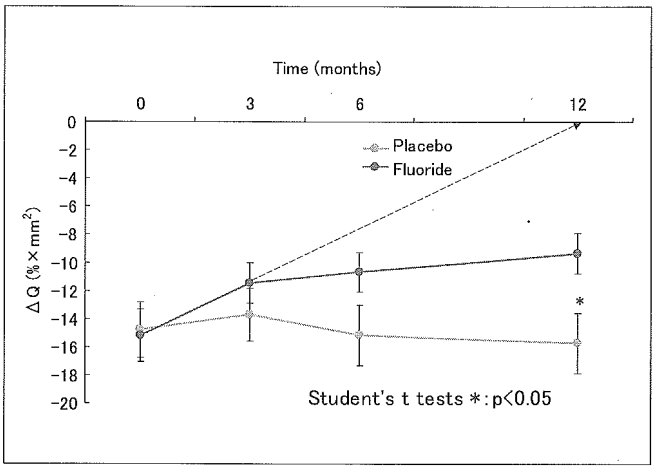

図14　コントロール群とフッ素配合歯磨剤群とのΔQにおける経時的変化

5．まとめ

齲蝕予防を実践するための技術，早期齲蝕検出法が完成すると，初期齲蝕の評価（進行・停止・回復）ができ，各歯に応じたテーラーメイド齲蝕予防治療が可能になる。また，現在行われている環境要因を中心とした齲蝕リスク評価にホスト要因を加えることができ，より，精度の高い齲蝕リスク評価を行うことができるようになる。さらに，齲蝕治療（充填処置，補綴処置）の二次齲蝕発現の有効性評価や新たな予防処置・剤の開発にもつながる可能性がある。

このように，早期齲蝕検出法は，歯の健康を獲得するための各種方面に影響を及ぼす可能性を持っており，歯科医療がEvidence-Basedな健康保持・予防へ転換するきっかけになることを信じてやまない。

引用文献

1) Early Detection of Dental Caries Ⅱ. Edited by G.K. Stookey, Proceedings of the 4 th Annual Indiana Conference, Indiana University School of Dentistry, 2000.
2) Early detection of Dental Caries Ⅲ. Indiana Conference, Indiana University School of Dentistry, Indianapolis, Indiana, 2003.
3) International Consensus Workshop on Caries Clinical Trials-Agreeing Were the Evidence Leeds, ICW-CCT Final Consensus Statements, April 2002.
4) Journal of Education；65, 2001.
5) Pitts, N. B.: Review of the ICW-CCT Meeting; Importance of Early Detection and the Philosophy & Approach of ICDAS: Early Detection of Dental Caries Ⅲ. Indiana Conference, 2003.
6) Pitts, N. B., Fejerskov, O., von der Fehr F. R.: Caries epidemiology, with special emphasis on diagnostic standards; in Dental Caries The disease and its clinical management, edited by O. Fejerskov and E. A. M. Kidd, Blackwell Munksgaard, UK, 141～164, 2003.
7) Verdonshot, E. H., Angmar-Mansson, B.: Advanced methods of caries diagnosis and quantification, in Dental Caries. The disease and its clinical management, edited by O. Fejerskov and E. A. M. Kidd, Blackwell Munksgaard, UK, 141～164, 2003.
8) 中島省志：海外での研究動向と最近の初期齲蝕の診断技術. The Nippon Dental Review, 63：150～154, 2003.
9) 飯島洋一：初期齲蝕の早期検出と脱灰・再石灰化評価. The Nippon Dental Review, 63：146～149, 2003.
10) 安藤昌俊：定量蛍光法（Quantitative Light-induced Fluorescence）による初期齲蝕検出. The Nippon Dental Review, 63：155～160, 2003.
11) 上村参生，神原正樹：早期齲蝕診断への機器応用の必要性. The Nippon Dental Review, 63：161～165, 2003.
12) Huysmans, M.D.N.J.M., Longbottom, C., Pitts, N.B.: Electrical methods in occlusal caries diagnosis: An *in vitro* comparison with visual inspection and bite-wing radiography. Caries Res, 32：324～329, 1998.
13) Peers, A., Hill, F. J., Mitropulos, C. M., Hollowat, P. J.: Validity and reproducibility of clinical examination, fibreoptic transillumination and bite-wing radiology for the diagnosis of small aproximal caries lesion: An *in vitro* study. Caries Res., 27：307～311, 1993.
14) Pinelli, C., Serra, M. C., Loffedo, L. C. M.: Validity and reproducibility of a laser fluorescence system for detecting the activity of white-spot lesions on free smooth surfaces *in vivo*. Caries Res., 36：19～24, 2002.
15) Angmar-Mansson, B., AI-Khateeb, A., Tranaeus, S.: Monitoring the caries process; Optical methods for clinical diagnosis and qualitification of enamel caries. Eur. J. Oral Sci., 104：480～485, 1996.
16) Bad, I.A., Feuerstein, O., Gazit, D.: Ultrasonic detector of approximal caries. Caries Res., 31, Abstract＃126, 1997.
17) Matsuyama,K., Nakashima, S., Kaneko, K.: An *in vitro* study on the detection of early enamel carious lesions by use of an infrared camera. Caries Res., 32, Abstract＃79, 1998.
18) Benedict, H.C.: Note on the fluorescence of teeth in ultraviolet rays. Science, 67：442, 1928.
19) Armstrong, W. G.: Fluorescence characteristics of sound and carious human dentine preparations. Arch. Oral Biol., 8：79～90, 1963.
20) Foreman, P. C.: The excitation of emission spectra of fluorescent components of human dentine. Arch. Oral Biol., 25：641～647, 1980.
21) Spitzer, D., ten Bosch, J. J.: The total Luminescence of bovine and human dental enamel. Calcif. Tissue Res., 20：201～208, 1976.
22) Uemura, M., Kambara, M.: Results of clinical trials of fluoride dentifrices using quantitative light fluorescence. Early Detection of Dental Caries Ⅲ, Indiana Conference, 2003.
23) 投稿中
24) 投稿中

Adsorption State of Egg Yolk PC Vesicles on Solid Colloidal Particles and Their Aggregation Behavior Induced by the Vesicle

Bo Yang,[†] Kunio Furusawa,[‡] and Hideo Matsumura*[,§]

Japan Society for the Promotion of Science (JSPS), Nanoarchitectonics Research Center, National Institute of Advanced Industrial Science and Technology (AIST), Tsukuba Central 5, 1-1-1 Higashi, Tsukuba Ibaraki 305-8562, Japan, Department of Chemistry, University of Tsukuba, Tsukuba, Ibaraki 305, Japan, and Life-electronics & Photonics, AIST, Tsukuba Central 2, 1-1-1 Umezono, Tsukuba, Ibaraki 305-8568, Japan

Received April 11, 2003

The state of egg yolk phosphatidylcholine (EPC) vesicles adsorbed on solid surfaces was evaluated by studying the aggregation behavior of the latex or silica particles with vesicles and the adsorption behavior of the vesicles on the surface. The aggregation behavior of latex and silica particle dispersions after adding EPC vesicles was studied using a dynamic light scattering method and optical microscopy. The adsorption of EPC vesicles on the solid particles was conducted by electrostatic attraction in a 10^{-4} M $LaCl_3$ aqueous solution. The amount of EPC adsorbed was determined by the depletion of EPC in the bulk solution. The state of EPC adsorbed was estimated by comparing the experimental and calculated results of the amount of EPC adsorbed. It was concluded that the EPC vesicles existed on the solid particle surface as a particle state, but not a bilayer membrane, and a "particle bridge" aggregation occurred at certain concentrations.

1. Introduction

Recently, various types of colloidal particles (for example, latex,[1−4] gold sol,[5−8] and dye[9,10] particles) have been introduced as sensor particles to immobilize the biorecognition element (for example, protein, DNA, etc.) in immunoassay and diagnosis. Because of the convenience and promptness of such colloid sensor particles, the research and development in this area have rapidly advanced in the medical treatment diagnosis. However, the bioelement may become inactive when it is immobilized directly on the colloidal particle surface. For example, membrane proteins will lose their activity when they leave the membrane. It is well-known that the vesicles possess the characteristics of a membrane and are easy to be modified with protein. They can be used as a protector for membrane proteins. Understanding the interaction between vesicles and colloid particles is important because the process involves the immobilization of vesicles on a colloid particle surface. In addition, it can also provide useful information about the interaction between the soft particles (vesicle) and solid particles in the colloid system.

We have been interested in the state or figures of lipid vesicles after they are adsorbed on various surfaces. In our previous work, the interactions between vesicles and a fluid surface, a flat oil/water interface, and emulsion droplets were reported.[11−13] It was shown that the adsorption behavior of the vesicles on the oil/water interface was governed by the van der Waals and electrostatic interactions. The vesicles first underwent gradual destruction on the oil/water interfaces and finally formed a monolayer-like structure. More recently, we have reported the possibility to make silica/vesicle/silica composite particles in a $LaCl_3$ aqueous solution using the silica particle as a template.[14] However, the details about the interactions between vesicles and solid colloid particles have not been reported yet. The objective of this work is to study the interactions between vesicles and solid surfaces by measuring the aggregation behavior of latex and silica particles after the L-α-phosphatidylcholine (PC) vesicles were added. In this work, the aggregation behavior of solid particles (latex and silica) and the amount of vesicle adsorbed on the particle surface were studied by employing various techniques, such as light scattering, electrophoresis and optical microscopy, and so forth.

2. Experimental Section

2.1. Materials. L-α-Phosphatidylcholine from egg yolk (EPC) (Sigma, product number 7318, approximately 98%) was pur-

* To whom correspondence should be addressed. Telephone: 81 298 61 5534. Fax: 81 298 61 5540. E-mail: hideo-matsumura@aist.go.jp.

† Japan Society for the Promotion of Science (JSPS), Nanoarchitectonics Research Center, National Institute of Advanced Industrial Science and Technology (AIST).

‡ University of Tsukuba.

§ Life-electronics & Photonics, AIST.

(1) Gribnau, T. C.; Leuvering, J. H.; van Hell, H. *J. Chromatogr.* **1986**, *376*, 175.
(2) Davalos-Pantoja, L.; Ortega-Vinuesa, J. L.; Bastos-Gonzalez, D.; Hidalgo-Alvarez, R. *J. Biomater. Sci., Polym. Ed.* **2000**, *11*, 657.
(3) Bohidar, H. B.; Bhakat, P.; Sharma, J.; Saxena, A. *Int. J. Biol. Macromol.* **2000**, *27*, 111.
(4) Molina-Bolivar, J. A.; Galisteo-Gonzalez, F.; Hidalgo-Alvarez, R. *J. Biomater. Sci., Polym. Ed.* **1998**, *9*, 1103.
(5) Pares, R. D.; Whitecross, M. I. *J. Immunol. Methods* **1982**, *51*, 23.
(6) Martin, J. M.; Paques, M.; van der Velden-de Groot, T. A.; Beuvery, E. C. *J. Immunoassay* **1990**, *11*, 31.
(7) Shyu, R. H.; Shyu, H. F.; Liu, H. W.; Tang, S. S. *Toxicon* **2002**, *40*, 255.
(8) Nir, J.; Lipert, R. J.; Dawson, G. B.; Porter, M. D. *Anal. Chem.* **1999**, *71*, 4903.
(9) Egger, D.; Bienz, K. *Methods Mol. Biol.* **1998**, *80*, 217.
(10) Watanabe, T.; Ohkubo, Y.; Matsuoka, H.; Kimura, H.; Sakai, Y.; Ohkaru, Y.; Tanaka, T.; Kitaura, Y. *Clin. Biochem.* **2001**, *34*, 257.
(11) Yang, B.; Matsumura, H.; Furusawa, K. *Colloids Surf., A* **1999**, *148*, 191.
(12) Yang, B.; Matsumura, H.; Furusawa, K. *Colloids Surf., B* **1999**, *14*, 161.
(13) Yang, B.; Matsumura, H.; Furusawa, K. *Langmuir* **2000**, *16*, 3160.
(14) Yang, B.; Matsumura, H.; Furusawa, K. *Langmuir* **2001**, *17*, 2283.

10.1021/la0301543 CCC: $25.00
Published on Web 09/18/2003

chased from Sigma Chemical Co., Ltd. (USA). It was used in our experiments without purification. The polystyrene latex particles used in this study were synthesized by the Kotera-Furusawa-Takeda method.[15] The diameter of the latex particle is 0.9 μm. The silica particle (size 1.0 μm in diameter) was kindly donated by Nippon Catalysis Co. Ltd. (Japan). The surface of these colloid particles was not rough and porous, as viewed by TEM and BET adsorption measurements. Other inorganic chemicals of analytical reagent grade were supplied by Wako Pure Chemical Industry (Japan). Water used in all the experiments was purified by the Nanopure system and redistilled in a Pyrex model still-1 (Iwaki Glass Co., Ltd., Japan).

2.2. Preparation of the Dispersions. Unilamellar EPC vesicles were prepared by the extrusion method according to Hope et al.[16] The mean diameter of the resulting vesicles is 0.2 μm, which was determined by a dynamic light scattering (DLS) apparatus (Otsuka Elect. ELS-800, Japan). This kind of EPC vesicle was utilized in our experiment due to the fact that it can give monodispersed EPC vesicles. The PC concentration was determined by the Bartlett method.[17] The silica dispersion was prepared by adding 1 g of silica powder into 500 mL of pure water and sonicating for 20 min. The concentration of the silica particles is approximately 5.1×10^8 piece/mL. A concentrated latex dispersion (0.5 mL, 2.4 wt %) was transferred into a flask containing 100 mL of pure water and was sonicated for 20 min. The concentration of the latex particles is about 4×10^8 piece/mL.

2.3. Analysis of Aggregation Behavior. The EPC vesicles were mixed with the latex or silica dispersions (v/v = 1) at different EPC vesicle concentrations. The mixing was achieved by a rapid mixing apparatus (MX-7, Union Giken. Co., Ltd., Japan), which has a jet device for rapid and controlled mixing. The mixtures were analyzed using the DLS apparatus (ELS-8000) immediately. We used the increasing diameter of aggregates as an indicator for the degree of aggregation. In detail, the aggregation behavior of latex or silica particles was evaluated by the enlarging size ratio (P) of the particle. P is given by $P = (D_t - D_0)/D_0$, where D_t is the mean diameter of the particles at time (t) after mixing EPC vesicles with latex or silica and D_0 is the mean diameter of the particles at the starting time ($t = 0$). In this case, DLS gives us an average diameter due to the polydispersion system. P values at 20 min after mixing the EPC vesicles with colloid particles were used to make the plot of P vs concentration of EPC vesicle added in system, because the virtual diameter of aggregates is almost constant over 20 min.

2.4. Electrophoresis. The electrophoretic measurements of EPC vesicles and other colloidal particles used in this study were carried out using the electrophoretic light scattering apparatus (ELS-8000) and microelectrophoresis (Zeecom, Microtec Co., Ltd., Japan).[18] ζ-Potentials were calculated from electrophoretic mobility data by using the O'Brien–White equation.[19] To prepare samples for electrophoresis, vesicles, latex, or silica were mixed with $LaCl_3$ aqueous solution. The vesicle–colloid particle (latex or silica) complex was separated from the mixture of vesicle and colloid particles by the ultrafiltration method (with a polycarbonate membrane filter, pore size 1.0 μm) after mixing for 20 min, and it was washed with a 10^{-4} M $LaCl_3$ aqueous solution until the EPC concentration in the washed elution was zero as determined by the Bartlett method.[17]

2.5. Adsorbed Amount of EPC Vesicles on Solid Particles. A solid suspension (1 mL) was mixed with 1 mL of an EPC vesicle dispersion, and the mixture was stirred for 4 h. The coagulated latex or silica particles were separated from the single vesicle particles by centrifugation for 30 min under 800g or 2000g, respectively. The phospholipid concentrations in the supernatant and original vesicle dispersion were determined by the Bartlett method.[17] The amount of EPC adsorbed on the solid particles was calculated from the mass balance.

(15) Kotera, A.; Furusawa, K.; Takeda, Y. *Kolloid Z. Z. Polym.* **1970**, *239*, 677.

(16) Hope, M. J.; Bally, M. B.; Webb, G.; Cullis, P. R. *Biochim. Biophys. Acta* **1985**, *812*, 55.

(17) Bartlett, G. R. *J. Biol. Chem.* **1959**, *234*, 466.

(18) Only the electrophoretic mobility of EPC vesicles was carried out using the electrophoretic light scattering apparatus because the size of EPC vesicles is too small ($D = 0.2$ μm) and cannot be observed by the microelectrophoresis.

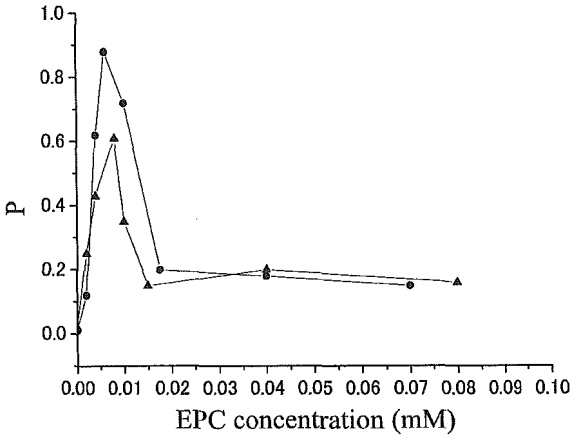

Figure 1. Plot of the enlarging rate of the solid particle size (P) vs the concentration of EPC in a 10^{-4} M $LaCl_3$ solution: (●) latex; (▲) silica.

Table 1. MAC and ζ-Potential Values for Latex and Silica Dispersions

system	MAC (mM)	ζ_{MAC}[a] (mV)	ζ_B[b] (mV)	ζ_S[c] (mV)
latex	0.006	+30	−22.5	+40
silica	0.008	+32	−37.5	+43

[a] ζ_{MAC} = the ζ-potential at the MAC. [b] ζ_B = the ζ-potential before addition of the EPC vesicle. [c] ζ_S = the ζ-potential at the adsorption saturation concentration of the EPC vesicle.

2.6. Optical Microscopy. The dispersions of solid particles (silica or latex) and EPC vesicles were mixed (1:1 v/v) using a rapid mixing apparatus (MX-7). After mixing for 20 min, a small amount of the mixture was transferred into a thin-wall glass cell. Subsequently, the sample cell was put on the microscope stage and the behavior of vesicles and the solid particles was observed with an optical microscope system (Olympas IMT-2 or BH 2), and the pictures were taken with a TV camera (Hamamatsu Photonics Co. Ltd., Japan).

All experiments were conducted at 25 ± 1 °C.

3. Results

3.1. Aggregation Behavior of Latex and Silica Dispersions Induced by Addition of EPC Vesicles. The enlarging size ratio (P) of latex and silica particles after adding EPC vesicles in these solid dispersions with various concentrations in a 10^{-4} M $LaCl_3$ aqueous solution is shown in Figure 1. $LaCl_3$ was chosen to control the surface charges of the vesicle and colloidal particles because $LaCl_3$ can give a higher positive charge at low concentration (high concentration is not good for vesicle stability) than NaCl and $MgCl_2$.[13] As can be seen in Figure 1, the P value of the latex aggregate increases with increasing EPC vesicle concentration, reaches the maximum at a certain concentration, and then decreases with a further increase of the EPC vesicle concentration. The concentration of EPC vesicles at which the maximum of the P value is achieved is called the "maximum aggregation concentration (MAC)". The same tendency was observed for the silica dispersion. The data of the MAC for each system are listed in Table 1.

Furthermore, the aggregation behaviors of the latex and silica dispersions were also observed directly using an optical microscope at three EPC vesicle concentrations: for latex (Figure 2), (a) [EPC] = 0 mM, (b) [EPC] = 0.006 mM (MAC), (c) [EPC] = 0.06 mM; for silica (Figure

(19) O'Brien, R. W.; White, L. K. *J. Chem. Soc., Faraday Trans.* **1978**, *74*, 1607.

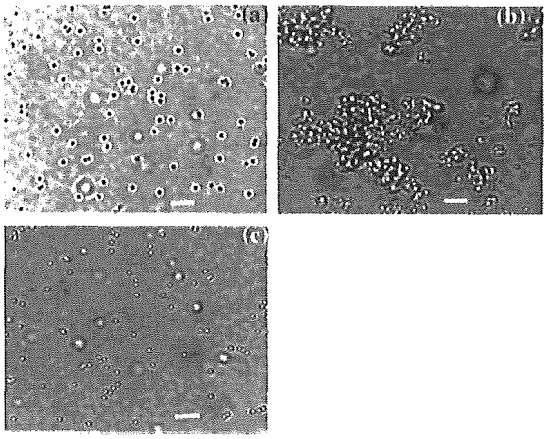

Figure 2. Photos of the aggregation behavior of latex particles at different EPC concentrations in a 10^{-4} M $LaCl_3$ solution: (a) [EPC] = 0; (b) [EPC] = 0.006 mM; (c) [EPC] = 0.06 mM. Scale bar = 5 μm.

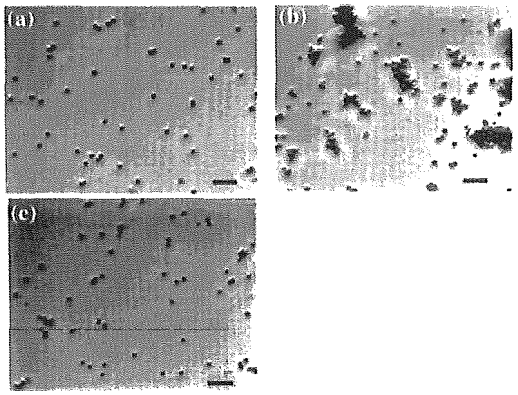

Figure 3. Photos of the aggregation behavior of silica particles at different EPC concentrations in a 10^{-4} M $LaCl_3$ solution: (a) [EPC] = 0; (b) [EPC] = 0.008 mM; (c) [EPC] = 0.08 mM. Scale bar = 5 μm.

3), (a) [EPC] = 0 mM, (b) [EPC] = 0.008 mM (MAC), (c) [EPC] = 0.08 mM. As shown in Figure 2a, in the absence of EPC vesicles, no aggregates of latex particles were observed, which is due to the electrostatic effect between the bare surfaces of particles. A large number of aggregates were found around the MAC (Figure 2b). However, at even higher EPC vesicle concentrations, latex aggregates were not found (Figure 2c). A similar trend was found for silica dispersions (Figure 3): that is, at [EPC] = 0, no aggregates of silica were observed (Figure 3a); at the MAC (0.008 mM), lots of aggregates of silica were found (Figure 3b); and over the MAC (0.08 mM), no aggregates of silica were found (Figure 3c).

3.2. Electrophoresis. The surface electrical properties of the different particles were investigated by measuring their electrophoretic mobility. The ζ-potentials were calculated using the electrophoretic mobility data. First, the ζ-potentials of the component particles (latex, silica particle, and EPC vesicles) were measured at various $LaCl_3$ concentrations. As shown in Figure 4, the negative ζ-potentials of EPC vesicles decreased with increasing $LaCl_3$ concentration and changed to positive values over a certain concentration. On the other hand, in the cases of latex and silica, the ζ-potentials decreased with the increase of $LaCl_3$ concentration and no sign change until $[LaCl_3] = 10^{-2}$ M. At $[LaCl_3] = 10^{-4}$ M, the value of the

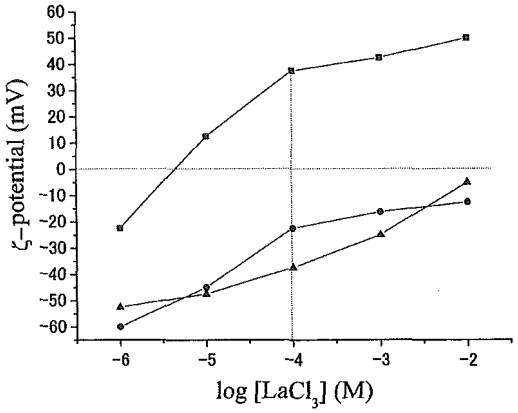

Figure 4. ζ-Potentials of the latex particle (●), silica particle (▲), and EPC vesicle (■) vs concentration of $LaCl_3$.

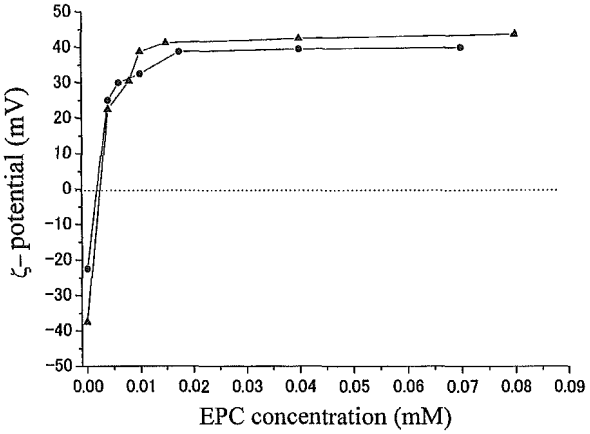

Figure 5. ζ-Potentials of the latex particle (●) and silica particle (▲) in a 10^{-4} M $LaCl_3$ solution as a function of EPC concentration.

ζ-potential for latex, silica, and EPC vesicles is −22.5, −37.5, and +37.5 mV, respectively.

Second, the ζ-potentials of latex and silica particles after the addition of EPC vesicles with various concentrations were measured in 10^{-4} M $LaCl_3$ (Figure 5). As can be seen in Figure 5, the ζ-potentials of latex and silica particles increased quickly from negative to positive values with increasing EPC concentration, which is due to the adsorption of positively charged EPC vesicles on latex and silica surfaces by electrostatic attraction. The data of the ζ-potentials of latex and silica at the MAC are summarized in Table 1.

3.3. Amount of EPC Vesicles Adsorbed on the Latex and Silica Surfaces. The amounts of EPC vesicles adsorbed on the latex and silica surfaces as a function of the EPC concentration are shown in Figure 6. The amount adsorbed is expressed by the number of phospholipid molecules adsorbed per square meter of latex and silica surface. The amount of EPC adsorbed on the latex surface increases with increasing EPC concentration and reaches a saturated value at a specific EPC concentration. A similar tendency was observed for silica particles. It is shown that the saturated value for latex or silica particles is $250 \times 10^{17}/m^2$ or $200 \times 10^{17}/m^2$, respectively.

4. Discussion

4.1. Form of EPC Vesicles Adsorbed on Latex and Silica Particles. As shown in Figure 4, the ζ-potential of EPC vesicles is a positive value (37.5 mV) at 10^{-4} M $LaCl_3$. But on the other hand, latex or silica particles have

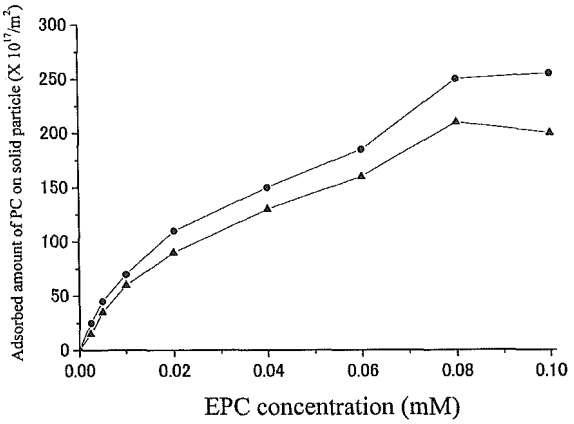

Figure 6. Adsorbed amount of EPC on the latex surface (●) and silica surface (▲) vs EPC concentration.

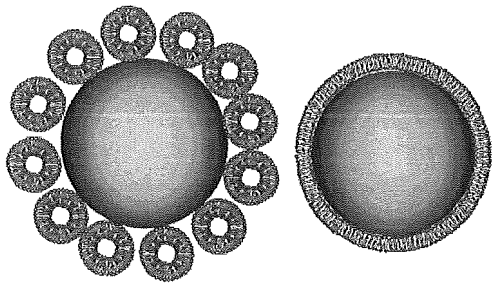

Figure 7. Two models for the EPC vesicles adhered on latex or silica particles: (a) a single vesicle layer model; (b) a lipid molecular bilayer model.

a negative ζ-potential of −22.5 or −37.5 mV, respectively. The results suggest that the positively charged EPC vesicles can be adhered strongly on the negatively charged latex or silica surface. This can be confirmed from the data of the ζ-potentials of latex and silica particles after the addition of EPC vesicles into these particle systems (Figure 5). In both cases the ζ-potentials changed quickly and showed a constant positive value over a specific EPC concentration.

There are two possible states for EPC vesicles adsorbed on the latex or silica surfaces: (1) a vesicle-particle layer (Figure 7a) and (2) a lipid molecular bilayer (Figure 7b). To clarify the adsorption state of the EPC vesicles, the amounts of EPC adsorbed on the latex and silica surfaces were measured and compared with the theoretically obtained values from the two models. For calculation, the area per EPC molecule is assumed to be 0.7 nm^2.[20] For the one single vesicle layer model, we assumed that the vesicles are of uniform size, having a unilamellar spherical shape. The analytical amounts of adsorption are indicated in Table 2. As can be seen, for latex surfaces, the theoretical value is 200 × $10^{17}/m^2$ from the one single vesicle layer model and 30 × $10^{17}/m^2$ from the single bilayer model. For silica surfaces, the theoretical adsorption amount is 160 × $10^{17}/m^2$ from the one single vesicle layer model and 25 × $10^{17}/m^2$ for the single bilayer model.

The saturated adsorbed amounts of EPC are close to and more than the values of the single vesicle layer model (Table 2 and Figure 6), which suggests that EPC vesicles

Table 2. Saturated Adsorption Amount of EPC on Latex and Silica Surface in 10^{-4}M $LaCl_3$ at 25 °C

system	vesicle particle layer model Γ ($10^{17}/m^2$)	molecular bilayer model Γ ($10^{17}/m^2$)	experimental Γ ($10^{17}/m^2$)
latex	200	30	250
silica	160	25	200

can be adsorbed on latex or silica surfaces as the vesicle particle layer (Figure 7a).

To further prove this, we measured the size of EPC vesicle/latex or EPC vesicle/silica composite particles directly by the DLS measurement. To determine the size of colloid particle/EPC vesicle composite particles exactly, it is preferred to be a monodisperse system. We used the ultrafiltration to remove the free PC vesicles. A 1.0 mM suspension of EPC vesicles (expressed by the EPC molecules concentration) was mixed with the latex or silica suspension, which was enough for covering the solid particles. Then, the EPC vesicle/latex or EPC vesicle/silica composite particles were separated from the free EPC vesicles by the ultrafiltration method with a polycarbonate membrane filter (pore size 1.0 μm), and the mean size of the composite particles was determined by DLS. We can get a monodisperse distribution graph in DLS measurements. The diameter is 1.33 μm for latex and 1.44 μm for silica. These values are close to 1.3 μm for latex and 1.4 μm for silica, which were calculated from the single vesicle particle layer model (Figure 7a). These results mean that the EPC vesicles are adsorbed on latex or silica particles as a spherical vesicular shape.

4.2. Mechanism of the Aggregation Behavior of Latex and Silica Particles Induced by Adding EPC Vesicles. Using the DLS (Figure 1) and optical microscopy results (Figure 2), the aggregation mechanism of latex (or silica) particles induced by addition of EPC vesicles has been analyzed. To understand the mechanism, electrophoresis measurements for latex and silica suspensions with addition of EPC vesicles having different concentrations were carried out. As shown in Figure 5, the ζ-potential of the solid particles decreased quickly with increasing EPC concentration and changed to positive values at a very low EPC concentration. In a 10^{-4} M $LaCl_3$ solution, the ζ-potential at the MAC is +30 mV for latex or +32 mV for silica, respectively (Table 1). Such a behavior of the ζ-potential is difficult to explain by a simple charge neutralization mechanism. According to this mechanism, the maximum aggregation of solid particles will occur at the charge neutralization point, that is, $\zeta = 0$. Therefore, the "particle bridge between latex (or silica) particles" induced by EPC vesicles must be taken into account. Since the EPC vesicles and the solid particles have opposite charges (EPC vesicle, $\zeta = +37.5$ mV; silica, $\zeta = -37.5$ mV; latex, $\zeta = -22.5$ mV), there should be an attractive force between the EPC vesicles adsorbed on solid particles and bare solid particles. Under these experimental conditions, the repulsive forces between solid particles can be ignored because the vesicle diameter ($D = 0.2$ μm) is much larger than the thickness of the electric double layer on the solid surface at 10^{-4} M $LaCl_3$. The thickness of the electric double layer is calculated as 12.4 nm using the method described in ref 21. The schematic image of "particle bridges" is shown in Figure 8. With the increases in the EPC concentration, the number of bridging sites increases. This results in a substantial increase in their aggregates (a). However, the negative charges on the solid particle

(20) Israelachvili, J. N.; Mitchell, D. J.; Ninham, B.W. *Biochim. Biophys. Acta* **1977**, *470*, 185.

(21) Israelachvili, J. N. *Intermolecular and surface force*; Academic Press: London, 1992; Chapter 12.

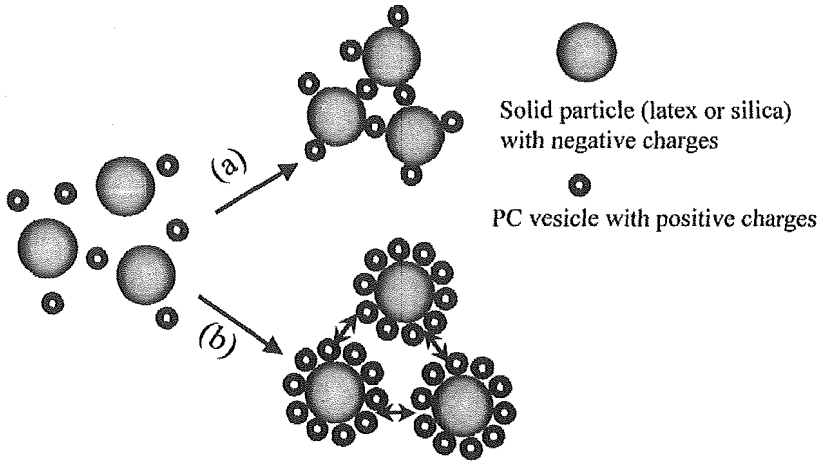

Figure 8. Schematic picture of the assembling behavior of the latex or silica particles after addition of EPC vesicles: (a) at low EPC vesicle concentration; (b) at high EPC vesicle concentration.

are neutralized gradually and finally reverse to a positive sign by the adsorption of EPC vesicles. In this situation, the attractive force between the adsorbed EPC vesicles and the bare solid surface becomes weak. When adsorption of EPC vesicles exceeds a certain value, the solid particle surfaces are covered with enough vesicles and show a positive charge. In this concentration range, the electrostatic repulsion between the EPC vesicle's layers on solid particles becomes predominant over the bridging effect and, hence, the aggregation is prevented.

5. Conclusions

The EPC vesicles adsorb on solid particle surfaces as a particle state and form the composite particles, which are covered by the EPC vesicle particles at high EPC concentration. The aggregation of solid particles with EPC vesicles is due to the "particle bridges" of vesicle particles between the solid particles.

LA0301543

ACADEMIC PRESS

Available online at www.sciencedirect.com
SCIENCE DIRECT®

Journal of Colloid and Interface Science 264 (2003) 95–100

JOURNAL OF
Colloid and
Interface Science

www.elsevier.com/locate/jcis

Characterization of silica-coated hematite and application to the formation of composite particles including egg yolk PC liposomes

Kunio Furusawa,* Hideo Matsumura, and Toshikazu Majima

National Institute of Advanced Industrial Science and Technology, Central-2, Umezono-1, Tsukuba, Ibaraki 305-8568, Japan

Received 27 September 2002; accepted 21 March 2003

Abstract

According to the method of Ohmori et al. (J. Colloid Interface Sci. 150 (1992) 594), a procedure is examined for the buildup of uniform silica layers on monodispersed hematite particles. It appears that the silica layer resulting is homogeneous and the layer thickness is controlled by the concentration of tetraethylorthosilicate (TEOS) in the medium. Further, egg PC liposomes, a typical biocolloid, are introduced onto the silica-coated hematite particle. The formation was proceeded by two types of processes: (1) heterocoagulation between the silica-coated hematite and egg PC liposomes by controlling the concentration of $LaCl_3$ in the medium, or (2) buildup using two proteins (lysozyme or cytochrome C) as binder molecules. These results were analyzed by zeta-potential measurements and a contact-type X-ray microscope, which is a unique technique for obtaining X-ray images of biological specimens in water with high resolution.

Keywords: Hematite; Silica; Coated particle; Composite particle; Core–shell particles; Lipid vesicles; PC liposome; Protein binder; Vesicle adsorption

1. Introduction

Recently, it was shown that inorganic or organic particles can be coated with other organic or inorganic layers with different chemical composition [1]; e.g., α-hematite [2], latex [3,4], and liposome particles [5] have been coated with silica layers. All the properties of the particles resulting have been altered to the same ones by the deposited silica layer. For example, by coating an ellipsoid of hematite(α-Fe_2O_3) with a silica layer, the resulting particles react as the silica particle, yet the particle is of anisometric shape, which cannot be produced with only silica by the usual preparation methods [2]. Usually the coating was conducted by precipitating the coating matter onto other particles dispersed in an aqueous medium once the system is supersaturated with the material. Alternately, the coating may form independently in a very fine dispersion and the composite may be produced by the heterocoagulation of the generated tiny particles with the suspended cores [6]. Obviously, the properties of the resulting composite particles will differ, depending on the mechanisms by which they are prepared.

In this study, a procedure is described for coating a uniform homogeneous silica layer on mono dispersed hematite particles. Iron oxides, which are of especial interest in magnetic recording, have been coated with silica in order to enhance their dispersibility in aqueous or nonaqueous media. In many cases, very small preformed silica particles were deposited on the magnetic cores [7,8]. Thus, the previously employed process differs from the coating technique developed in the present work.

Furthermore, in the present work, egg yolk phosphatidylcholine (PC) liposomes, a typical biocolloid, are introduced into silica-coated hematite particles as one component. In the preparation of these composite particles, two bioproteins (lysozyme and cytochrome C) were used as binder molecules. So the composite particles developed here can be used in the biomedical field as diagnostic and treatment medicine, because egg PC liposome and protein are biocompatible materials.

2. Experimental

2.1. Preparation of hematite cores

Polyhedral or cubic-type hematite (α-Fe_2O_3) particles were synthesized using the same method as Matijevic and

* Corresponding author.
E-mail address: furusawa-k@muh.biglobe.ne.jp (K. Furusawa).

0021-9797/03/$ – see front matter
doi:10.1016/S0021-9797(03)00313-8

co-workers [9,10]; i.e., aqueous solutions of $4–50\times10^{-3}$ mol/dm^3 $FeCl_3$ were aged for 3 days at 100 °C in a Pyrex bottle. The settled particles were washed and centrifuged several times to remove any extraneous ions. Among them, two kinds of hematite samples with diameters of 0.8 μm and 1.0 μm were mainly used as core particles.

2.2. Coating process

Hematite particles were coated with a silica layer using the hydrolysis of tetraethylorthosilicate(TEOS) by the process described earlier [2]. However, in order to determine the conditions for formation of uniform shells, the range of reactant concentrations was tested exactly.

A typical successful preparation procedure was as follows: to a 2-propanol solution of 0.45 mol/dm^3 ammonia and 3.05 mol/dm^3 water, a certain amount of hematite particles (e.g., 50 mg/dm^3) was added under agitation with a magnetic bar in a 100 cm^3 test tube. The tightly screw-capped container was then placed into a constant-temperature bath of 40 °C and equilibrated for 30 min. After the dispersion reached to a uniform temperature, $2–30\times10^{-3}$ mol/dm^3 TEOS solution was rapidly added and aged at 40 °C for varying periods of time (10–20 h) in order to produce different thicknesses of the coating layer.

2.3. Reagents

Two types of globular protein were used; lysozyme (Lsz, Sigma Co. Ltd., No. L-6876, isoelectric point at pH 11.4) from hen's egg and cytochrome C (CC, Boehringer GmbH, Mannheim, No. 103888, isoelectric point at pH 10) from horse heart. All inorganic chemicals were analytical reagent grade.

For the preparation of the aqueous solutions, we used distilled and deionized water, produced by an autostill system (WG240 Yamato Co.).

2.4. Liposome preparation

Egg yolk phosphatidylcholine (PC) was purchased from Sigma Chemical Co.,USA. The PC sample includes a small amount of acidic impurities, which are indicated by the negative electrophoretic mobility of its liposome [11]. Unilamellar PC liposomes were prepared by the extrusion method according to Hope et al. [12]. The mean diameter of the resulting liposomes was determined by a light-scattering apparatus (Otsuka Elect. ELS-8000). In this study, PC liposomes of 0.2 μm were used.

2.5. Synthesis and detection of coated particles

The adsorption of proteins was allowed to take place for 1.5–2 h at 0.1–0.2 mg/ml Lsz or CC solution using a dilute coated-particle suspension ($\phi = 0.0001$) and a saturated concentration without any free protein that was determined by mobility measurements of the coated particles was selected for treatments. Prior to mobility measurement, each suspension was further diluted to 1/10 using the same salt solution as the medium. So very low concentrations of protein and particles are achieved. During the adsorption and composite-formation process, suspensions of core (or coated) particles were mixed slowly by means rotating them end over end for 1–2 h.

The electrophoretic mobilities of core (or coated) particles and composite particles were measured using a microelectrophoretic apparatus (Rank Brothers Mark 2). The observed mobility (u) was converted to the ζ potential using the Smoluchowski equation.

The coated state and stability of composite particles were observed directly by an optical microscope. Furthermore, the morphological details of the coated (composite) particles were detected by a contact type X-ray microscope system.

2.6. X-ray microscope system

Silica-coated hematite and its composite particles with PC liposomes were imaged directly by contact-type soft X-ray microscopy using CR-39 plastics (PMMA) and readouted with AFM. The details of the sample preparation and the procedure were followed in the previously published way [13].

3. Results and discussion

3.1. Properties of hematite particles and particles coated with silica layers

Figure 1 shows a typical electron micrograph of hematite particles used in this study. The particles are semicubic or polyhedral in shape, and the ratio between the weight and the number averages of particle radius never exceeds 1.5. The particles formed are monocrystalline and exhibit the crystallographic features of α-Fe_2O_3.

The hematite particles were coated with a layer of silica by hydrolysis of tetraethylorthosilicate(TEOS) [2]. In Fig. 2, a typical electron microphotograph of coated particle is displayed. As seen from the figure, it is realized that the particles were covered with a uniform silica layer, instead of deposited particle layers.

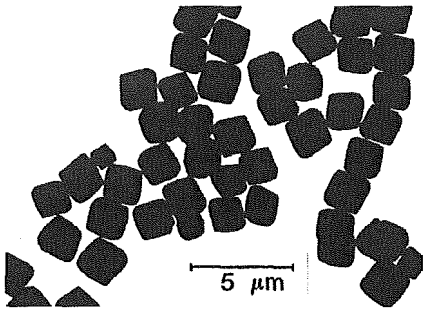

Fig. 1. Electron micrograph of α-Fe_2O_3 (hematite) particles.

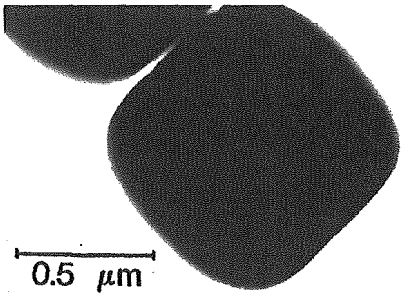

Fig. 2. Electron micrograph of composite particles (hematite/silica).

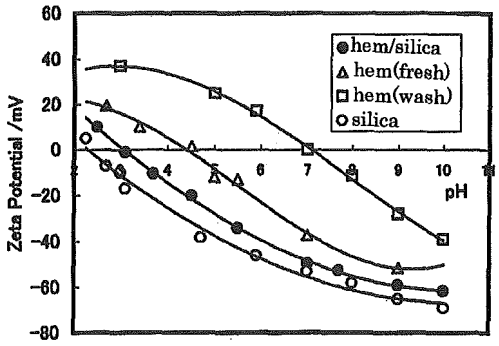

Fig. 3. ζ potentials of fresh hematite (△), washed hematite (□), hematite/silica (●), and silica (○) particles vs pH curves under 10^{-4} mol/dm^3 NaCl solution.

In Fig. 3, the typical ζ potentials of the fresh hematite particle and the coated particle with a silica layer are plotted against the medium pH. It is shown that the bare hematite particle has an isoelectric point (pH^0) at pH 4–5 and the pH^0 value was shifted gradually to the alkaline side by washing [14]. It is indicated that some ionic impurities (maybe Cl^-) were incorporated into the particles and was removed gradually from the surface by extensive washing. Furthermore, it is found that the original hematite particles would like to be flocculated gradually with elapsed time. On the other hand, the coated-hematite particles have been kept in the dispersed state for a long time and indicated at a fixed isoelectric point (pH^0 7). An example of the dispersed state is given by the photograph in Fig. 4. It is seen further that the dispersed state is almost the same for a few months and each particle included continues in rapid Brownian motion. Figure 3 also shows the electrophoretic mobilities of the silica particles prepared by the Stöber method [15]. The coated-hematite particle shows almost the same pH^0 as silica particles. Consequently, the coated particles exhibit the same properties as the silica in terms of surface potential and dispersibility.

3.2. *Multilayer formation by controlling the concentration of $LaCl_3$*

As the next stage, the formation of multilayers of hematite/silica/liposome has been examined. In this preparation, electrostatic attraction between original component particles

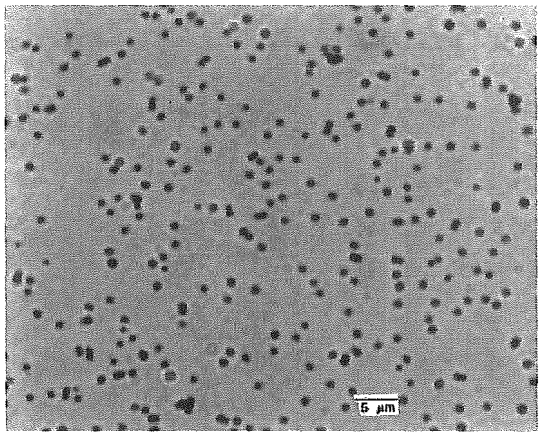

Fig. 4. Microphotograph showing the dispersed state of (hematite/silica) particles under 10^{-4} mol/dm^3 NaCl solution.

has been taken into account as the driving force. It is important that the egg PC liposome and the silica-coated hematite particles have opposite charges. We can control the surface charges of these particles by adjusting the concentration of $LaCl_3$ in the medium [11]. In Fig. 5, the ζ potential of egg PC liposomes and silica-coated hematite particles are shown as a function of $LaCl_3$ concentration. The ζ potential of the egg PC vesicle decreases with increasing $LaCl_3$ concentration and changes from negative to positive over 10^{-5} mol/dm^3 $LaCl_3$. This is due to the binding of La^{3+} ions to the phospholipid head group [16]. On the other hand, the ζ potential of silica-coated hematite remained negative over the whole concentration range of $LaCl_3$ studied. So egg PC liposome and silica-coated hematite have opposite signs of ζ potential at 10^{-4} mol/dm^3 $LaCl_3$ and a strong electrostatic attraction operated between them. Therefore, we selected $LaCl_3 = 10^{-4}$ mol/dm^3 as the salt concentration for heterocoagulation.

The heterocoagulation of these particles has been conducted as follows. A definite hematite/silica suspension con-

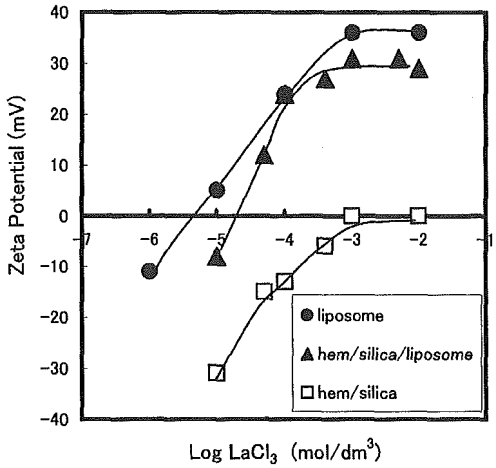

Fig. 5. ζ potentials of hematite/silica (□), hematite/silica/liposome (▲), and liposome (●) vs $LaCl_3$ concentration curves at pH 5.

trolled at a fixed $LaCl_3$ concentration was prepared. Then, on top of this vesicle suspensions controlled at the same $LaCl_3$ concentration were carefully added. After rotating end over end for 30 min, the system was left to stand for 1–2 h at room temperature to age the heterocoagulated particles. After that, free PC vesicles were removed by filtration (pore size, 1-μm filter) and washed several times with the same concentrated $LaCl_3$ solution. The ζ potential of heterocoagulates was measured under various $LaCl_3$ solutions. The results are presented as a function of $LaCl_3$ concentration in Fig. 5, as well as the data on the egg PC vesicles. As may be seen, a reversal of charge is observed in both the samples, and the pH^0 in the heterocoagulated system occurs at about 10^{-5} mol/dm^3 $LaCl_3$, which is not so different from the pH^0 of the single egg PC liposomes. Furthermore, according to analytical experiments with PC concentration after adsorption on silica and direct observation of the heterocoagulated particles by using a special optical microscopy, it is concluded that the vesicle form will be kept on the silica surface after heterocoagulation [11]. All these results indicate that heterocoagulation between the hematite/silica and egg PC liposome surely occurred in 10^{-4} mol/dm^3 $LaCl_3$ solution and hematite/silica/liposome composite particles were synthesized under this medium condition.

3.3. *Multilayer formation using protein binders*

As the second stage of composite formation, build-up using two protein binders was conducted. As the binders cytochrome C (CC) and lysozyme (Lsz) were used, because the pH^0's of these proteins are located at pH 10–11 [17] and electrostatic attraction between PC vesicles and silica-coated hematite can be expected after binding by these proteins. Protein binding was conducted by the usual end-over-end mixing. Here, an important condition is that the protein binder should be as low as possible because the residual molecules in the solution will adsorb directly onto the PC liposome and will influence on the composite formation. Here, all the experiments have been carried out under 0.1–0.3 mg/ml, because as shown in Fig. 6, both the proteins show saturated adsorption around at ~0.2 mg/ml. Figures 7 and 8 show the typical results of ζ potential changes on alternating addition of CC or Lsz and excess PC liposomes on negatively charged silica-coated hematite. The change of ζ potential is substantial; i.e., the highly negative ζ potentials of the original hematite/silica particle become positive after addition of protein binders and again return to negative values by treatment with the PC liposome. Figure 7 shows the ζ potential cycles, when Lsz was used as the binder molecule under two pH conditions (pH 4.3 and 7) of the medium. Also, Fig. 8 shows the ζ potential change when CC was used as the binder under pH 5.7 and 6.9, where all the protein concentrations was fixed at ~0.2 mg/ml, respectively. It appears that the scattering of experimental conditions hardly influences the cyclic behavior and in all systems the protein molecules play a role in new composite formation as binders.

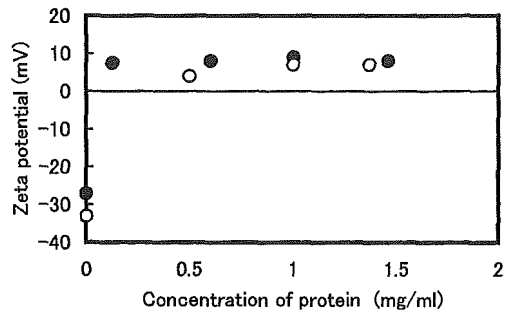

Fig. 6. Protein concentration vs ζ potential of (hematite/silica) curves which were treated under different protein concentrations (●, Lsz; ○, CC) in pH 5–7 aqueous solution.

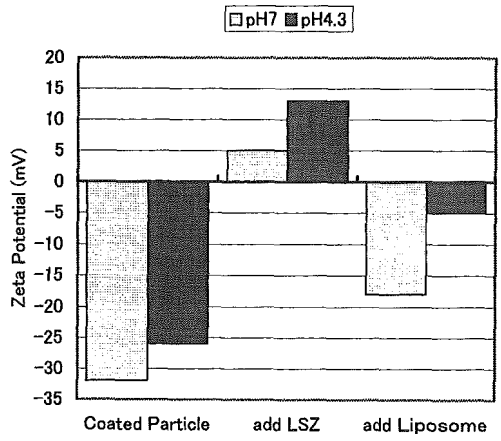

Fig. 7. ζ potential change with alternate addition of Lsz (□, pH 7; ■, pH 4.3) and PC liposome under 10^{-4} mol/dm^3 NaCl solution.

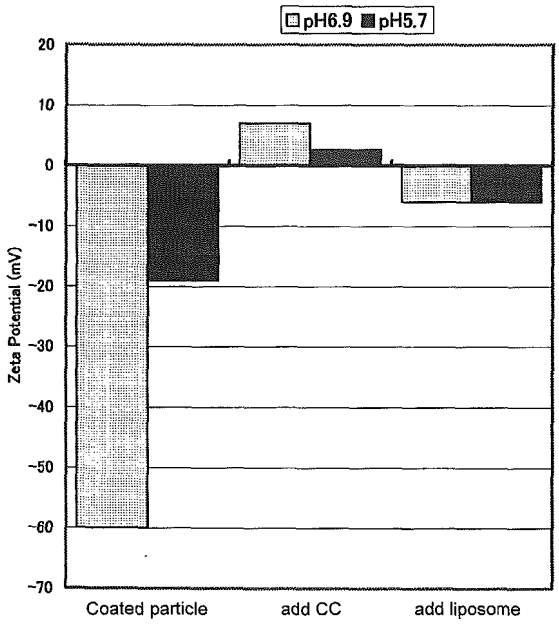

Fig. 8. ζ potential change on alternate addition of CC (□, pH 6.9; ■, pH 5.7) and PC liposome under 10^{-4} mol/dm^3 NaCl solution.

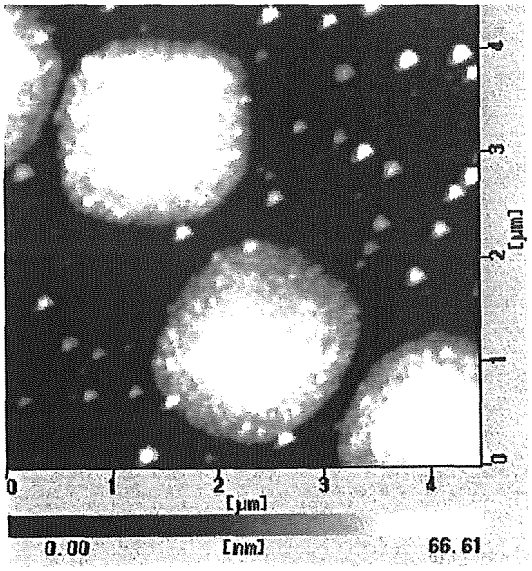

Fig. 9. X-ray microphotograph of (hematite/silica) particles.

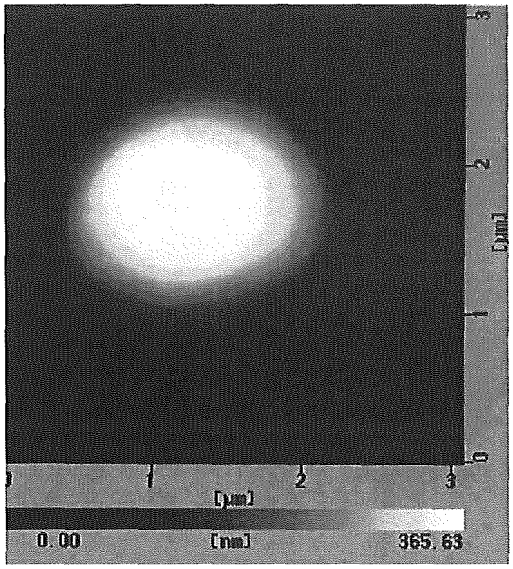

Fig. 10. X-ray microphotograph of (hematite/silica/liposome) particles.

Furthermore, it is known that the composite particles resulting here will be interesting in the biomedical field for diagnostic and treatment, because the PC liposome and protein molecule used here are typical biocolloids and biocompatible.

3.4. X-ray microscopy for the composite particles

Figures 9 and 10 show typical X-ray microphotographs of hematite/silica and hematite/silica/liposome particles prepared in the present experiment. The chamber used here allows preparation of fully hydrated samples, so our composite, including PC liposome, can be expected to keep its vesicle form on its surfaces [12]. As seen from Fig. 9, an X-ray micrograph of hematite/silica is constructed from a two-layer structure. The inner layer will be the hematite particle and the outer will be the silica layer. Although isolated small silica particles can be detected on the outside, it is clear from Fig. 9 that the hematite/silica is composed of a uniform silica layer and not of heterocoagulates of tiny particles. On the other hand, an X-ray micrograph of hematite/silica/liposome (Fig. 10) is constructed from a three-layer structure: (1) a light cloudy shadow covered on the composite from its outside, (2) a grayish layer of 20–30 nm surrounding the core region, (3) a brilliant white core seen in the center of the composite. These three layers would indicate the existence of three components in the particle, be egg PC liposome, silica, and α-hematite. The existence of protein binder cannot be detected. Also from Fig. 10, we cannot detect the existence of spherical relief similar to that of the original vesicles. The reason cannot be understand, but this X-ray microphotograph would indicate a lot of new knowledge and suggestions on the structure and formation mechanism for multilayer composite particles.

4. Conclusion

It appears that by choosing the concentration of TEOS and the reacting temperature, homogeneous silica layers with different thickness can be deposited on α-hematite particles. Furthermore, two kinds of formation process of multilayer composite particle including egg PC liposomes have been investigated:

(1) Egg PC liposome is coated on the hematite/silica particle based on the heterocoagulation mechanism by controlling the concentration of $LaCl_3$ in the medium;
(2) The buildup technique for these components has been applied by using two protein molecules (cytochrome C and lysozyme) as binders.

These results were analyzed by ζ potential measurements and contact-type X-ray microscopy.

References

[1] K. Furusawa, O.D. Velev, Colloids Surf. A 159 (1999) 359.
[2] M. Ohmori, E. Matijevic, J. Colloid Interface Sci. 150 (1992) 594.
[3] K. Yoshinaga, F. Nakashima, T. Nishi, Colloid Polym. Sci. 277 (1999) 136.
[4] K. Nagai, Y. Ohshi, K. Ishiyama, K. Kuramoto, J. Appl. Polym. Sci. 18 (1989) 2183.
[5] I.A. Banerjee, S. Gomes, Q. Wang, A.E. Ostafin, Adv. Mater. 12 (2000) 1291.
[6] K. Furusawa, C. Anzai, Colloids Surf. 63 (1992) 103.
[7] A. Garg, E. Matijevic, J. Colloid Interface Sci. 126 (1988) 243.
[8] A.M. Homola, M.R. Lorenz, H. Sussnerand, S. Rice, J. Appl. Phys. 61 (1987) 3898.
[9] M. Ozaki, S. Kratohvil, E. Matijevic, J. Colloid Interface Sci. 102 (1984) 146.
[10] E. Matijevic, P. Scheiner, J. Colloid Interface Sci. 63 (1978) 509.